JACS
JOURNAL OF THE AMERICAN CHEMICAL SOCIETY

ARTICLE

pubs.acs.org/JACS

Glycolaldehyde as a Probe Molecule for Biomass Derivatives: Reaction of C—OH and C═O Functional Groups on Monolayer Ni Surfaces

Weiting Yu, Mark A. Barteau, and Jingguang G. Chen*

Catalysis Center for Energy Innovation, Department of Chemical Engineering, University of Delaware, Newark, Delaware 19716, United States

Supporting Information

ABSTRACT: Controlling the activity and selectivity of converting biomass derivatives to syngas (H_2 and CO) is critical for the utilization of biomass feedstocks as renewable sources for chemicals and fuels. One key chemistry in the conversion is the selective bond scission of the C—OH and C═O functionalities, which are present in many biomass derivatives. Because of the high molecular weight and low vapor pressure, it is relatively difficult to perform fundamental surface science studies of C6 sugars, such as glucose and fructose, using ultrahigh vacuum techniques. Glycolaldehyde ($HOCH_2CH{=}O$) is the smallest molecule that contains both the C—OH and C═O functional groups, as well as the same C/O ratio as C6 sugars, and thus is selected as a probe molecule in the current study to determine how the presence of the C═O bond affects the reaction mechanism. Using a combination of density functional theory calculations and experimental measurements, our results indicate that the reaction pathway of glycolaldehyde to produce syngas can be enhanced by supporting monolayer Ni on a Pt substrate, which shows higher activity than either of the parent metals. Furthermore, the Pt substrate can be replaced by tungsten monocarbide to achieve similar activity and selectivity, indicating the possibility of using Ni/WC to replace Ni/Pt as active and selective catalysts with higher stability and lower cost.

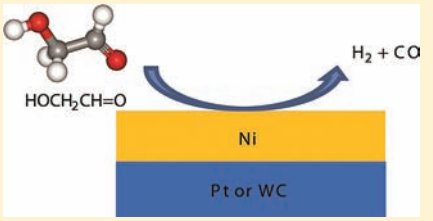

1. INTRODUCTION

Biomass-derived molecules are a promising class of alternative energy resources because they offer the advantages of being widely available, renewable, and potentially carbon-neutral. Such molecules generally contain more oxygen atoms than are found in petroleum-based feedstocks. Previously, Dumesic and co-workers[1] studied aqueous-phase reforming of small oxygenates such as ethylene glycol over different transition metals. Their work demonstrated that the ethylene glycol reforming activity followed the order of Pt > Ni > Ru > Rh > Pd > Ir and the H_2 selectivity decreased in the order of Pd > Pt > Ni > Ru > Rh. Overall, Pt was identified as one of the most promising monometallic catalysts for small oxygenate reforming with both high activity and H_2 selectivity.

Bimetallic surfaces and catalysts are known to often exhibit unique properties different from either of the parent metals.[2−6] For example, two bimetallic configurations have been previously identified for the Ni/Pt surfaces. The subsurface PtNiPt(111) structure, representing a monolayer of Ni atoms residing underneath the Pt top layer,[7] was found to bond adsorbates more weakly than either Ni or Pt, responsible for a novel low-temperature hydrogenation pathway for the C═C and C═O bonds.[8] In contrast, the surface NiPtPt(111) configuration,[9,10] with one layer of Ni atoms on the top of the Pt(111) substrate,[7] was identified to bind adsorbates more strongly than either Ni or Pt, leading to a higher reforming activity for small oxygenates, including ethanol, ethylene glycol, and glycerol.[9,10]

The study of small alcohols and polyols has illustrated the possibility of using single crystal surfaces to determine the bond scission mechanisms of the C—OH moiety.[11] However, different from the small alcohols and polyols, the C═O functional group is also present in the ring-opened structures of C6 sugars. Because of the high molecular weight and low vapor pressure, it is relatively difficult to perform fundamental surface science studies of C6 sugars using ultrahigh vacuum (UHV) techniques. Glycolaldehyde ($HOCH_2CH{=}O$), the smallest molecule that contains both C—OH and C═O bonds as well as the same C/O ratio as C6 sugars, is selected as a probe molecule in the current study to determine how the presence of the C═O functional group affects the reaction mechanism. To the best of our knowledge, the current work represents the first time that glycolaldehyde, with both C—OH and C═O functionalities, is studied as a model compound of biomass derivatives on catalyst surfaces. The current study combines density functional theory (DFT) calculations and experimental verification using temperature-programmed desorption (TPD) and high-resolution electron energy loss spectroscopy (HREELS).

The reaction pathways of glycolaldehyde are also investigated on Ni-modified tungsten monocarbide (WC) surfaces to compare the similarities and differences between Ni/WC and NiPtPt(111). According to a previous study,[12] the favorable NiPtPt(111) bimetallic structure for reforming is not stable at high temperatures due to the diffusion of surface Ni atoms into the Pt bulk.[7] WC has been reported in the literature[13−17] to possess electronic properties similar to those of Pt. Moreover, WC has been reported to be an

Received: September 18, 2011
Published: November 08, 2011

effective barrier for preventing diffusion of the topmost metal layer,[18] as verified by the thermal behavior of Ni/WC.[19] Therefore, the reaction of glycolaldehyde is studied on the Ni/WC surfaces to determine the feasibility of using Ni/WC as a less expensive and more thermally stable reforming catalyst to replace Ni/Pt.

2. THEORETICAL AND EXPERIMENTAL METHODS

2.1. DFT Calculations. All DFT calculations in this work were performed with the Vienna Ab initio Simulation Package (VASP).[20−22] The PW91 functional[23] was used in the generalized gradient approximation (GGA).[24] Details about the calculation procedures are similar to those described previously[17] and are provided in the Supporting Information.

Glycolaldehyde was adsorbed on the atop sites of adjacent metal atoms. The optimized geometry on the NiPtPt(111) surface is shown in Figure 1a,b as an example. Glycolaldehyde binding energy (BE) is related to the interaction between the surface and glycolaldehyde molecule,and was calculated using the equation:

$$BE_{glycolaldehyde/slab} = E_{glycolaldehyde/slab} - E_{slab} - E_{glycolaldehyde}$$

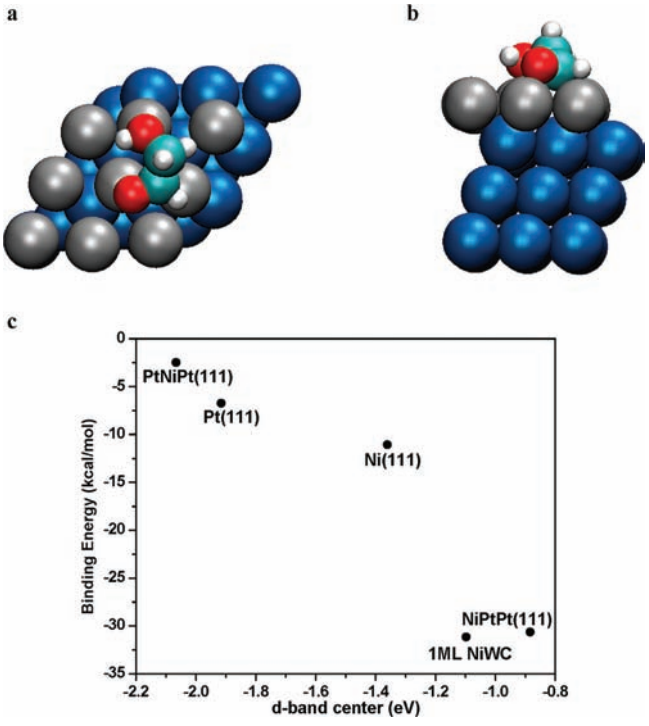

Figure 1. (a) Top and (b) side views of adsorption geometry of glycolaldehyde on NiPtPt(111) and (c) the correlation between the surface d-band center and glycolaldehyde binding energy on different surfaces (Pt, blue; N, gray; C, aqua; O, red; H, white).

where $E_{glycolaldehyde/slab}$ is the total energy of the slab plus the adsorbed glycolaldehyde molecule, and E_{slab} and $E_{glycolaldehyde}$ are the energies of the bare slab and free glycolaldehyde molecule, respectively.

2.2. Experimental Techniques. Glycolaldehyde (Fisher Scientific, 98%, dimer) was transferred into glass sample cylinders and purified using repeated heat−pump−cool cycles. All other gases, oxygen, hydrogen, neon, ethylene, and carbon monoxide, were of research purity and used without further purification. The purity of all the reagents was verified prior to experiments using mass spectrometry. The glycolaldehyde sample was preheated to 330 K and dosed to the UHV system through a stainless steel dosing tube approximately 10 cm away from crystal surface. Details about the surface preparation and TPD/HREELS measurements are similar to those described previously[17] and are provided in the Supporting Information.

3. RESULTS

3.1. DFT Calculations on Ni/Pt(111) Surfaces. The binding energies of glycolaldehyde on Pt(111), NiPtPt(111), PtNiPt(111), and Ni(111) surfaces were calculated using DFT. Figure 1c displays the correlation between the surface d-band center and the binding energy of glycolaldehyde on each surface. Glycolaldehyde binding energy is found to increase as the surface d-band center moves closer to the Fermi level, consistent with the theory of chemisorption by Hammer and Nørskov.[25] The O−M bond distances of glycolaldehyde in the optimized bonding configurations are calculated and listed in Table 1. The trend of O−M bond lengths on the different surfaces follows the order of PtNiPt(111) > Pt(111) > Ni(111) > NiPtPt(111). Generally, the surface with the shortest O−M bond length shows the highest glycolaldehyde binding energy. In a previous study of ethylene glycol reforming on different Pt-based bimetallic surfaces, a volcano relationship was observed between the binding energy of ethylene glycol and its reforming activity.[26] The four surfaces in the current study, PtNiPt(111), Pt(111), Ni(111) and NiPtPt(111), were all on the left-hand side of the volcano curve, leading to the conclusion that the surface with the highest binding energy should exhibit the highest reforming activity. As shown in Figure 1c, the NiPtPt(111) bimetallic structure is found to exhibit the highest glycolaldehyde binding energy among the four surfaces and thus is predicted to have the highest activity.

3.2. Glycolaldehyde TPD on Ni/Pt(111) Surfaces. Possible net reaction pathways of glycolaldehyde are summarized as follows:

$$a\mathrm{HOCH_2CHO} \rightarrow 2a\mathrm{C_{ad}} + 2a\mathrm{O_{ad}} + 2a\mathrm{H_2} \quad (1)$$

$$b\mathrm{HOCH_2CHO} \rightarrow 2b\mathrm{CO} + 2b\mathrm{H_2} \quad (2)$$

$$c\mathrm{HOCH_2CHO} \rightarrow c\mathrm{C_2H_4} + 2c\mathrm{O_{ad}} \quad (3)$$

Table 1. Binding Energies and Bond Lengths of Glycolaldehyde and Its Initial Intermediate on Different Surfaces

	$H^{\#1}OCH_2CH^{\#2}O$			$^{\#1}OCH_2CH^{\#2}O$		
surfaces	BE (kcal/mol)	$^{\#1}$O−M (Å)	$^{\#2}$O−M (Å)	BE (kcal/mol)	$^{\#1}$O−M (Å)	$^{\#2}$O−M (Å)
PtNiPt(111)	−2.47	2.50	2.19	−27.20	2.06	2.25
Pt(111)	−6.73	2.38	2.10	−38.06	2.01	2.09
Ni(111)	−11.06	2.15	1.90	−59.69	1.96	1.89
NiPtPt(111)	−30.63	2.03	1.90	−70.83	1.82	1.88
1ML NiWC	−31.14	2.10	1.91	−69.84	1.89	1.93

dx.doi.org/10.1021/ja208786f |J. Am. Chem. Soc. 2011, 133, 20528–20535

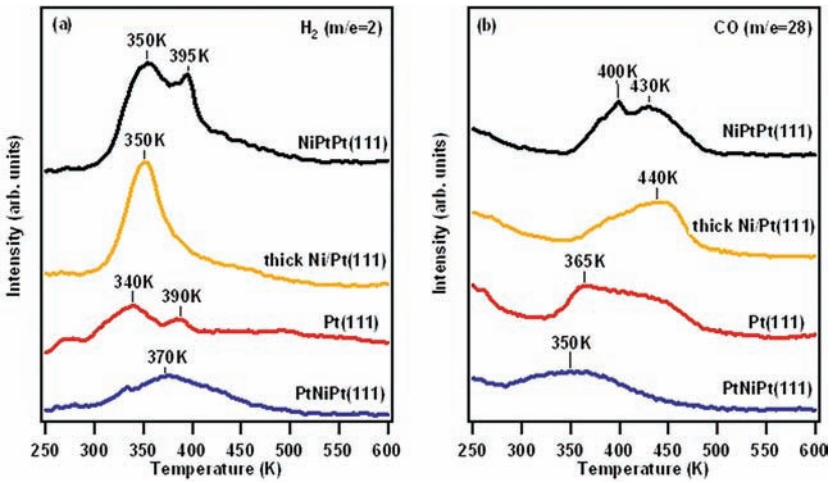

Figure 2. TPD spectra of (a) H_2 and (b) CO following 4L glycolaldehyde exposure on different surfaces.

Table 2. Quantification of TPD Results of Glycolaldehyde Reaction Pathways on Pt(111) and Ni/Pt(111) Surfaces

	activity (molecule per metal atom)			selectivity (%)	
	reforming	total decomposition			total
surface	(b)	(a)	total	reforming	decomposition
NiPtPt(111)	0.191	0.004	0.195	98	2
thick Ni/Pt(111)	0.171	0.000	0.171	100	0
Pt(111)	0.133	0.000	0.133	100	0
PtNiPt(111)	0.114	0.000	0.114	100	0

Reaction 1 represents the total decomposition pathway, producing H_2, as well as C_{ad} and O_{ad} that remain on the surface. Reaction 2 is the reforming pathway involving the C—C bond scission with the C—O/C═O bonds remaining intact, which is the most desirable pathway as it produces syngas. Reaction 3 is the deoxygenation pathway that selectively dissociates the C—O/C═O bonds to produce ethylene. Here values of *a*, *b*, and *c* represent the amount of chemisorbed glycolaldehyde that undergoes each reaction pathway, and can be calculated as follows:

$$H_2 \text{ yield} = 2a + 2b \Rightarrow a = 0.5 * H_2 \text{ yield} - b \quad (4)$$

$$\text{CO yield} = 2b \Rightarrow b = 0.5 * \text{CO yield} \quad (5)$$

$$C_2H_4 \text{ yield} = c \Rightarrow c = C_2H_4 \text{ yield} \quad (6)$$

The yields of H_2, CO, and C_2H_4 were determined from the TPD peak areas, as described below. Figure 2 displays the TPD spectra from Pt(111) and Ni/Pt(111) bimetallic surfaces after an exposure of 4L glycolaldehyde. The molecular desorption of glycolaldehyde from the four surfaces occurs at around 200K (not shown). Figure 2 compares the TPD spectra of the reaction products, H_2 and CO. In Figure 2a, the decomposition of glycolaldehyde leads to the desorption of H_2 at 350 and 395 K from NiPtPt(111), 350 K from thick Ni/Pt(111), 340 and 390 K from Pt(111), and 370 K from PtNiPt(111). Two desorption peaks of the CO product are observed between 350 and 440 K, with the exact temperature depending on the specific surface. No desorption peaks are observed at m/e = 26 and m/e = 27, indicating there is no ethylene produced on Ni/Pt(111) surfaces. The detection of both H_2 and CO confirms the production of syngas from glycolaldehyde from all four surfaces. Comparing the desorption temperatures in Figure 2 to those from the adsorption of H_2 or CO (spectra not shown), the desorption of the H_2 product appears to be reaction-limited, while that of the CO product is desorption-limited.

In order to quantify glycolaldehyde activity following each reaction pathway, the yields of H_2 and CO products were obtained by comparing their TPD peak areas with those after saturation exposures of H_2 and CO on Pt(111). In the quantification, the literature saturation coverages of H_2 (0.45ML[27]) and CO (0.68ML[28]) on Pt(111) were used. The yield of C_2H_4 was calibrated by comparing the mass spectrometer sensitivity factor at equal background concentrations of C_2H_4 and CO.

The quantification of the amount of glycolaldehyde undergoing each reaction pathway was obtained using eqs 4−6. Table 2 summarizes the activity and selectivity of glycolaldehyde decomposition on the four surfaces. The NiPtPt(111) surface shows the highest reforming activity and total activity, followed by thick Ni/Pt(111), Pt(111), and PtNiPt(111) surface, which is consistent with the DFT predicted trend in Figure 1c. The activity trend for glycolaldehyde is also similar to that of ethylene glycol[10] on the corresponding Ni/Pt(111) surfaces.

3.3. Glycolaldehyde HREELS on Ni/Pt(111) Surfaces. The HREELS measurements were performed to identify the reaction intermediates of glycolaldehyde. Figure 3 compares the HREEL spectra of glycolaldehyde on clean Pt(111) and NiPtPt(111) surfaces. In Figure 3a, the vibrational features at 115 K are assigned to the following vibrational modes of glycolaldehyde,[29,30] as summarized in Table 3: τ(OH), 744 cm^{-1}; ν(CC), 852 cm^{-1}; ν(CO), 1089 cm^{-1}; $\delta(CH_2)$, 1394 cm^{-1}; ν(C═O), 1718 cm^{-1}; $\nu_s(CH_2)$, 2875 cm^{-1}; and ν(OH), 3450 cm^{-1}. Overall, the observation of these modes suggests that glycolaldehyde adsorbs molecularly on the Pt(111) surface at 115 K with the O−H bond intact. There is almost no change in the vibrational features of glycolaldehyde after heating to 150 K. After heating to 175 K, the sharp ν(C═O) peak at 1718 cm^{-1} becomes broader and shifts to lower frequency, suggesting that the C═O functional group in glycolaldehyde starts to interact with the Pt(111) surface at 175 K, most likely through a di-σ configuration. Upon heating to 200 K, the τ(OH) mode at 744 cm^{-1} disappears, indicating the O−H bond scission of the adsorbed glycolaldehyde. The ν(OH) mode

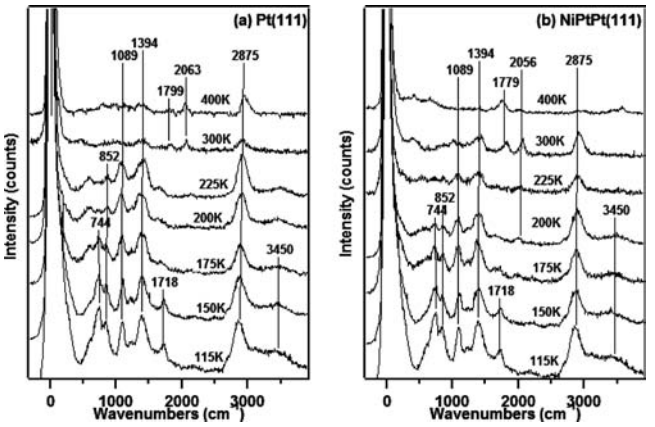

Figure 3. HREEL spectra of 1L glycolaldehyde on (a) Pt(111) and (b) NiPtPt(111) surfaces.

Table 3. Vibrational Assignment of Glycolaldehyde

	frequency (cm^{-1})			
mode	vapor[a]	solid[a]	on Pt(111)[b]	on WC[b]
τ(OH)	752	753	744	758
ν(CC)	859	863	852	866
ν(CO)	1112	1109	1089	1096
$\delta(CH_2)$	1425	1423	1394	1427
ν(C═O)	1754	1747	1718	1745
$\nu_s(CH_2)$	2840	2858	2875	2902
ν(OH)	3549	3313	3450	3301

[a] References 29 and 30 [b] This work.

at 3450 cm^{-1} is not used as an indicator of the O−H bond scission in glycolaldehyde because the adsorption of water from the UHV background during the HREELS experiments also produces ν-(OH) modes in this frequency range. No change is observed when the surface is heated from 200 to 225 K. When the Pt(111) surface is further heated to 300 K, the ν(CC) mode at 1089 cm^{-1} disappears, indicating the cleavage of the C−C bond between 225 and 300 K. This is consistent with the presence of the CO product at 1799 and 2063 cm^{-1}, adsorbed on the surface through bridge and atop sites, respectively. After the surface is heated to 400 K, most vibrational modes associated with glycolaldehyde disappear, with the remaining features being characteristic of those of surface hydrocarbon fragments.

As shown in Figure 3b, glycolaldehyde adsorbs molecularly on the NiPtPt(111) surface at 115K, as indicated by the presence of the τ(OH) mode at 744 cm^{-1} and the other characteristic modes (see Table 3). The spectral development at higher temperature is very similar to that observed on Pt(111), with the onset of di-σ bonding at the C═O moiety at 175 K and the dissociation of the O−H bond at 225 K. One noticeable exception is that the ν(CC) mode at 852 cm^{-1} almost completely disappears at 225 K, which is lower in temperature than that on the clean Pt(111) surface. Another difference is that the intensities of the hydrocarbon fragments are nearly absent on NiPtPt(111) at 400 K, with the only surface species being the linear and bridge-bonded CO product from the glycolaldehyde decomposition.

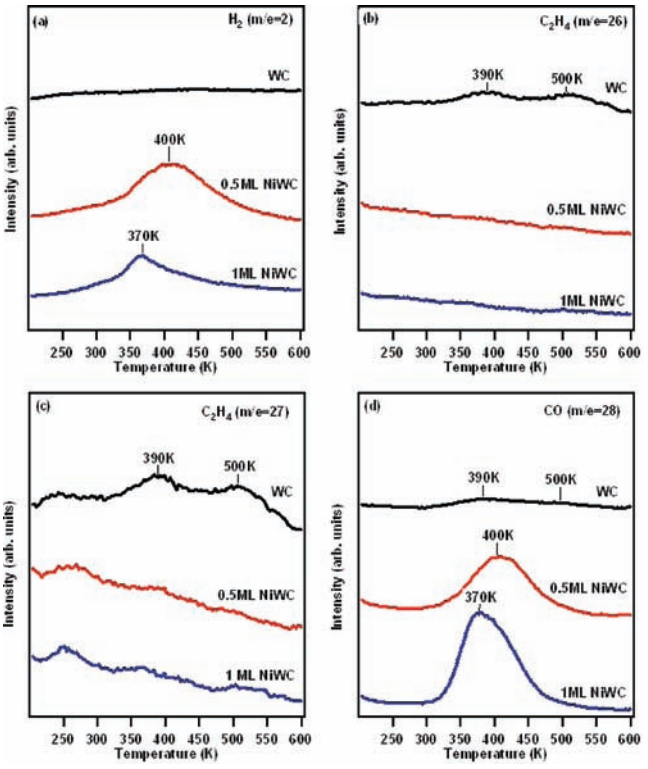

Figure 4. TPD spectra of (a) H_2, (b) C_2H_4 (m/e = 26), (c) C_2H_4 (m/e = 27), and (d) C_2H_4/CO (m/e = 28) with 4L glycolaldehyde exposure on clean WC and Ni/WC surfaces.

3.4. DFT Calculations on 1ML NiWC Surface. As stated in the Introduction, supporting monolayer Ni on WC instead of Pt offers the advantages of higher thermal stability and lower cost. As shown in Figure 1c, the binding energy of glycolaldehyde on the 1ML NiWC surface is very close to that on the NiPtPt(111) surface, confirming the general similarity between the WC and Pt substrates. As shown in Table 1, the calculated O−M bond lengths on the 1ML NiWC surface (2.10 and 1.91 Å) are also very similar to the corresponding values on NiPtPt(111) (2.03 and 1.90 Å). On the basis of the similarities of glycolaldehyde binding energies and O−M bond distances on the two surfaces, the 1ML NiWC surface is predicted to have activity toward glycolaldehyde similar to that of the NiPtPt(111) surface.

3.5. Glycolaldehyde TPD on WC and Ni/WC Surfaces. Glycolaldehyde TPD experiments were performed on clean and Ni-modified WC surfaces exposed to 4L glycolaldehyde. In Figure 4a, the H_2 desorption peak is not observed from the clean WC surface. From Figure 4d, two m/e = 28 desorption peaks are observed on the WC surface at 390 and 500 K, with peaks desorbing at the same temperatures for m/e = 26 and m/e = 27. The peaks in Figure 4b−d are the cracking patterns of ethylene, indicating that glycolaldehyde reacts on the WC surface through the C—O/C═O bond scission. Desorption peaks are observed at 400 K for 0.5ML NiWC and 370 K for 1ML NiWC in Figure 4d, with no corresponding desorption peak detected from Ni-modified WC surfaces at m/e =26 and m/e = 27, indicating that ethylene is not produced on Ni-modified WC surfaces and the desorption peaks in Figure 4d are from the CO product. Combining with the production of H_2 in Figure 4a, the TPD results indicate that glycolaldehyde reacts on Ni-modified WC surfaces to produce H_2 and CO,

Table 4. Quantification of TPD Results of Glycolaldehyde Reaction Pathways on WC and Ni/WC Surfaces

	activity (molecule per metal atom)	
surface	reforming (b)	deoxygenation (c)
WC	0.000	0.016
0.5ML NiWC	0.116	0.000
1ML NiWC	0.187	0.000

exhibiting the same reaction pathways as on Ni/Pt(111) surfaces.

Similar quantification procedures stated in section 3.2 are applied here for glycolaldehyde reaction on WC and Ni-modified WC surfaces. On the clean WC surface, all glycolaldehyde molecules undergo the deoxygenation pathway to produce ethylene by breaking both the C═O and C—O bonds while keeping the C−C bond intact. As shown earlier in the deoxygenation pathway in eq 3, all the hydrogen atoms in glycolaldehyde molecule are transferred to ethylene and no hydrogen is produced, consistent with the absence of the H_2 TPD peak from WC in Figure 4a.

The quantification of the TPD results is compared in Table 4. The 1ML NiWC surface exhibits the highest reforming activity. More importantly, similar glycolaldehyde reforming activity is observed on the 1ML NiWC and NiPtPt(111) surfaces, consistent with the DFT prediction based on the similar binding energies of glycolaldehyde on the two surfaces.

3.6. Glycolaldehyde HREELS on WC and Ni/WC Surfaces. The HREELS spectra of 1L glycolaldehyde on clean WC and 1ML NiWC surfaces are shown in Figure 5. The spectrum on WC at 100 K (Figure 5a) shows the characteristic vibrational features of molecularly adsorbed glycolaldehyde, as summarized in Table 3. After heating of the surfaces to 200 K, the τ(OH) mode at 758 cm^{-1} disappears, indicating the O−H bond cleavage. The ν(C═O) mode at 1745 cm^{-1} also disappears, demonstrating that the bonding occurs through the di-σ bond at the C═O moiety at 200 K. On the clean WC surface, the glycolaldehyde spectra remain similar between 200 and 400 K. Upon heating to 500 K, the intensities of all the vibrational features start to decrease and almost completely disappear at 600 K, consistent with the detection of the ethylene product between 400 and 600 K in the TPD spectra (Figure 4).

The HREEL spectra of glycolaldehyde on 0.5ML WC (not shown) and 1ML NiWC (Figure 5b) surfaces are very similar, and therefore 1ML NiWC surface is shown as a representative of Ni-modified WC surfaces. As summarized in Table 3, the spectrum following 1L glycolaldehyde exposure on the 1ML WC surface at 100 K is characteristic of molecularly adsorbed glycolaldehyde with the O−H bond intact. Upon heating to 200 K, both the τ(OH) mode at 758 cm^{-1} and the ν(C═O) mode at 1745 cm^{-1} disappear, indicating the O−H bond scission and the bonding through a C═O di-σ configuration. No change is observed when the 1ML NiWC surface is heated from 200 to 300 K. After heating to 400 K, the ν(CC) mode at 866 cm^{-1} disappears completely, indicating C−C bond cleavage between 300 and 400 K. This is consistent with the TPD results in Figure 4 that both H_2 and CO products desorb at 370 K from the reaction of glycolaldehyde on the 1ML NiWC surface. The desorption temperature is higher than that of molecularly adsorbed CO (at ~290 K), indicating that the desorption of the CO product from glycolaldehyde is reaction-limited and corresponds to the C−C bond scission temperature.

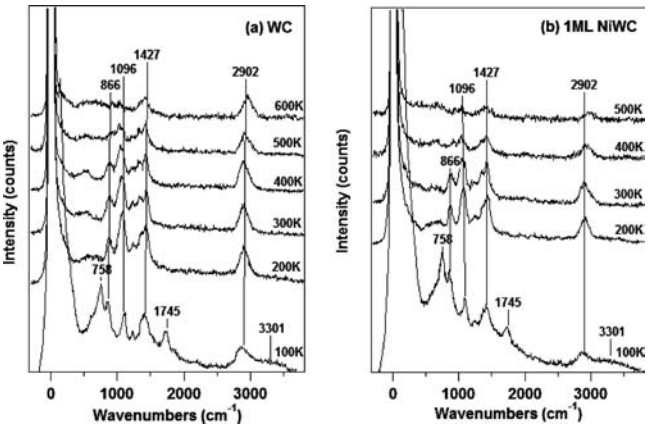

Figure 5. HREEL spectra of 1L glycolaldehyde on (a) WC and (b) 1ML NiWC surfaces.

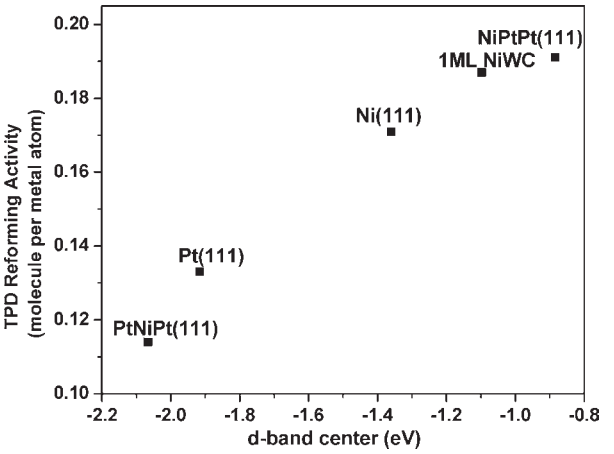

Figure 6. Correlation between the surface d-band center and glycolaldehyde TPD reforming activity on different surfaces.

4. DISCUSSION

4.1. Glycolaldehyde Reaction on Ni/Pt(111) Surfaces. From the DFT calculations in Table 1, the binding energies of glycolaldehyde and its reaction intermediate from the O−H bond scission, OCH_2CHO, follow the trend of NiPtPt(111) > Ni(111) > Pt(111) > PtNiPt(111). As shown in Figure 1c, the binding energies increase as the surface d-band center moves closer to the Fermi level. The quantification results from TPD experiments (Table 2) reveal that the activity of glycolaldehyde on these surfaces follows the same trend with the binding energy and d-band center correlation, with the NiPtPt(111) surface exhibiting the highest reforming activity and total activity. These results suggest that, similar to those reported for small alcohols and polyols, the binding energy and the surface d-band center can be used as descriptors to predict the trend in glycolaldehyde activity.

According to Figure 6, there is a nearly linear correlation between the surface d-band center and the reforming activity derived from the TPD experiment, in which the surfaces with

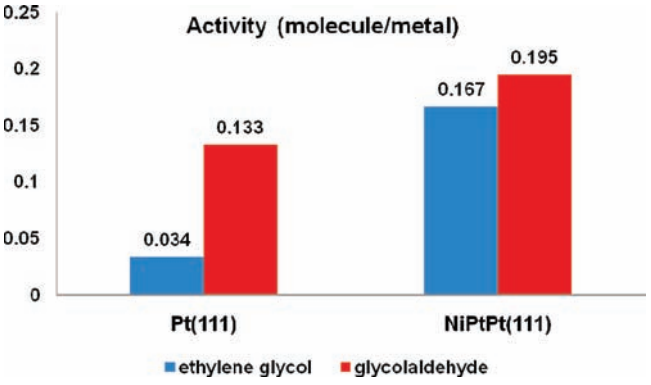

Figure 7. Comparison of the activity from TPD measurements of ethylene glycol and glycolaldehyde on Pt(111) and NiPtPt(111) surfaces.

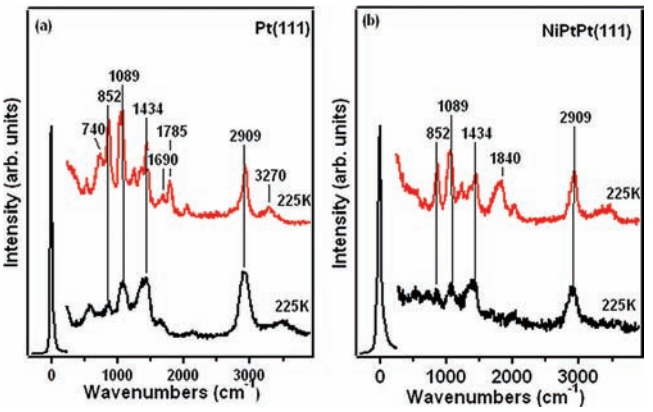

Figure 8. Comparison of HREEL spectra of reaction intermediates from ethylene glycol (top spectrum) and glycolaldehyde (bottom spectrum) on (a) Pt(111) and (b) NiPtPt(111) surfaces.

d-band center closer to the Fermi level exhibit the higher reforming activity. Due to the availability of the values of surface d-band center for a wide range of monometallic and bimetallic surfaces,[4] the correlation in Figure 6 should provide useful information on selecting catalysts with desirable reforming activity of glycolaldehyde and potentially other biomass-derived oxygenates with the C═O functionality.

Based on the HREELS results, there are general similarities in the decomposition sequence of glycolaldehyde on the clean Pt(111) and NiPtPt(111) surfaces: (1) Glycolaldehyde is molecularly adsorbed on both surfaces at 115 K with O−H bond intact. (2) After heating the surfaces to 175 K, the ν(C═O) mode becomes broader and shifts to lower frequency, indicating the bonding of glycolaldehyde to the surfaces through a di-σ η(C,O) bond in the C═O moiety, consistent with the optimized DFT binding configuration of glycolaldehyde on both surfaces, as shown in Figure 1a,b. (3) The O−H bond scission occurs after the formation of the di-σ bonded glycolaldehyde, at the temperatures between 175 and 225 K, most likely producing an OCH_2CHO surface intermediate. (4) Upon heating to 300 and 400 K, only vibrational modes associated with hydrocarbon fragments and the CO product remain on the surface. These similarities in glycolaldehyde surface bonding configuration and bond scission sequence are confirmed by the same reaction products observed in the TPD spectra in Figure 2.

The main difference between the Pt(111) and NiPtPt(111) surfaces is that the ν(CC) mode at 852 cm^{-1} disappears between 225 and 300 K on Pt(111), while the C−C bond scission is nearly complete on NiPtPt(111) by 225 K. The more facile C−C bond scission on NiPtPt(111) than on Pt(111) is most likely responsible for the higher reforming activity on the NiPtPt(111) surface (see Table 2).

4.2. Influence of C═O Functionality on Oxygenate Decomposition. In the current study, glycolaldehyde is used as a probe molecule for C6 sugars to determine the decomposition pathway of molecules with both C—OH and C═O functionalities. In order to understand the influence of the C═O bond, a comparison between glycolaldehyde and ethylene glycol on Ni/Pt(111) surfaces is made in this section. It is found that both glycolaldehyde and ethylene glycol[10] react on Ni/Pt(111) surfaces to produce syngas. In addition, the activities of the two molecules follow the same trend of NiPtPt(111) > thick Ni/Pt(111) > Pt(111) > PtNiPt(111).

A comparison of the activities of ethylene glycol (EG) and glycolaldehyde on Pt(111) and NiPtPt(111) surfaces is shown in Figure 7. The activity of EG is much lower than that of glycolaldehyde on Pt(111), while the difference is much smaller on the NiPtPt(111) surface. This observation suggests that the presence of the C═O functional group affects the rate determining step of C2 oxygenates on Pt(111). As described in a previous study of EG decomposition on Pt(111),[31] the first reaction step involves a facile cleavage of one of the O−H bonds to form a $HOCH_2CH_2O$ intermediate. This is followed by the C−H bond scission to produce a glycolaldehyde intermediate and then the scission of the second O−H bond. In contrast, the decomposition of glycolaldehyde on Pt(111) does not require the C−H scission step, which should in turn lead to a higher reforming activity than that of EG.

Such difference is confirmed by the HREELS measurements, as compared in Figure 8 for EG and glycolaldehyde following a common annealing temperature of 225 K on both Pt(111) and NiPtPt(111). On Pt (111) (Figure 8a), the vibrational spectrum of the reaction intermediate of EG (upper spectrum) is consistent with the formation of a glycolaldehyde-like intermediate from the scission of an O−H bond and a C−H bond, as indicated by the presence of the τ(OH) mode at 740 cm^{-1} and the ν(C═O) modes at 1690 and 1785 cm^{-1}. In comparison, at the same annealing temperature the intermediate of glycolaldehyde (lower spectrum) already undergoes the O−H bond scission and di-σ bonding through the C═O functional group, as confirmed by the absence of the τ(OH) mode, as well as the significant reduction in intensity and a shift in frequency ν(C═O) mode. The HREELS results indicate that, at a common temperature of 225 K, the intermediate from glycolaldehyde interacts more strongly than that of EG on Pt(111). Overall, the comparison of Figure 7 and 8a suggests that the presence of the C═O functionality enhances the interaction on Pt(111), leading to a higher reforming activity of glycolaldehyde than EG.

In contrast, the reaction intermediates from EG and glycolaldehyde appear to be similar on the NiPtPt(111) surface (Figure 8b). The absence of the τ(OH) mode indicates that the O−H bonds in both EG and glycolaldehyde undergo complete scission on NiPtPt(111) at 225 K. This is consistent with previous DFT prediction that the first reaction intermediate of EG is produced through the scission of both O−H bonds on NiPtPt(111).[31] Overall, the comparison in Figure 7 and 8b suggests that, for surfaces that show high activity toward the O−H bond scission, such as NiPtPt(111), the presence of the

C═O functionality does not significantly affect the decomposition pathways of the C2 oxygenates.

4.3. Similarities between Monolayer Ni on WC and Pt(111) Substrates. According to the HREEL spectra of glycolaldehyde on the 1ML NiWC surface (Figure 5), glycolaldehyde is molecularly adsorbed at 100 K, and is converted to a di-σ η(C,O) configuration. The O−H scission is also observed at 200 K, indicating that the reaction intermediate is likely OCH_2CHO. Overall, the HREELS results of glycolaldehyde on 1ML NiWC are similar to those on NiPtPt(111), consistent with the similar reaction pathways from the TPD results from the two surfaces (Table 2). These experimental results are consistent with DFT predictions that the 1ML NiWC and NiPtPt(111) surfaces exhibit very similar glycolaldehyde binding energies, O−M bond lengths, and the surface d-band center values. These results confirm the hypothesis that the Pt substrate can be replaced by WC to support 1ML Ni. Considering the higher thermal stability and lower cost of 1ML NiWC, it is a promising catalyst for the reforming of biomass-derived oxygenate molecules to produce syngas.

The HREELS and TPD results also reveal that glycolaldehyde follows different reaction pathways on clean WC and Ni modified WC surfaces. On the clean WC surface, the C−C bond of the OCH_2CHO intermediate is intact up to 400 K (Figure 5). The intensity of the ν(CC) feature only starts to decrease at the temperature range corresponding to the desorption of ethylene in the TPD measurements (Figure 4). These results indicate that the clean WC surface preferentially decomposes the C—O/C═O bonds in oxygenates while keeping the C−C bond intact, suggesting the possibility of using WC as a preferential deoxygenation catalyst.

Finally, although Figure 6 shows a qualitative correlation between the reforming activity of glycolaldehyde on Ni/Pt and Ni/WC surfaces and the surface d-band center values, which are typically related linearly to binding energy, detailed comparison of the activation barriers for glycolaldehyde decomposition on these surfaces is required to understand the origin of such correlation. In particular, a detailed understanding the activation barriers and reaction networks of glyolaldehyde decomposition on the monolayer Ni/Pt(111) and Ni/WC surfaces would provide important insight into the similarities and/or differences between Pt and WC in facilitating the bond scission mechanisms.

5. CONCLUSIONS

In the current study, glycolaldehyde is used as a probe molecule for biomass derivatives with both C—OH and C═O functionalities. The following conclusions can be made from the combined DFT prediction and experimental verification using TPD and HREELS:

(1) For the reaction of glycolaldehyde, NiPtPt(111) shows the highest reforming activity and total activity among the Ni/Pt(111) surfaces. The activity trend found in experiments is consistent with the DFT prediction based on binding energy, suggesting that binding energies and surface d-band center values can be used as descriptors to predict the activity of glycolaldehyde on catalytic surfaces.

(2) Based on the comparison of the activity and reaction intermediates of EG and glycolaldehyde, the presence of the C═O functionality enhances the activity on the Pt(111) surface. On the other hand, for surfaces with high activity toward the O−H bond scission, such as NiPtPt(111), the presence of C═O does not significantly affect the activity or reaction pathway of C2 oxygenates.

(3) Monolayer Ni surfaces supported on WC and Pt(111) show similar glycolaldehyde reforming activity, indicating that monolayer Ni/WC may be preferable to Ni/Pt as active and selective catalysts for biomass reforming with higher stability and lower cost.

■ ASSOCIATED CONTENT

Supporting Information. Preparation and characterization of monolayer Ni surfaces; detailed description of theoretical and experimental methods. This material is available free of charge via the Internet at http://pubs.acs.org.

■ AUTHOR INFORMATION

Corresponding Author
jgchen@udel.edu

■ ACKNOWLEDGMENT

This article was based on work supported as part of the Catalysis Center for Energy Innovation, an Energy Frontier Research Center funded by the U.S. Department of Energy, Office of Science, Office of Basic Energy Sciences, under Award No. DE-SC0001004.

■ REFERENCES

(1) Davda, R. R.; Shabaker, J. W.; Huber, G. W.; Cortright, R. D.; Dumesic, J. A. *Appl. Catal., B* **2003**, *43*, 13.
(2) Berlowitz, P. J.; Goodman, D. W. *Surf. Sci.* **1987**, *187*, 463.
(3) Berlowitz, P. J.; Houston, J. E.; White, J. M.; Goodman, D. W. *Surf. Sci.* **1988**, *205*, 1.
(4) Chen, J. G.; Menning, C. A.; Zellner, M. B. *Surf. Sci. Rep.* **2008**, *63*, 201.
(5) Goodman, D. W. *Ultramicroscopy* **1990**, *34*, 1.
(6) Rodriguez, J. A. *Surf. Sci. Rep.* **1996**, *24*, 225.
(7) Kitchin, J. R.; Khan, N. A.; Barteau, M. A.; Chen, J. G.; Yakshinksiy, B.; Madey, T. E. *Surf. Sci.* **2003**, *544*, 295.
(8) Murillo, L. E.; Goda, A. M.; Chen, J. G. *J. Am. Chem. Soc.* **2007**, *129*, 7101.
(9) Skoplyak, O.; Barteau, M. A.; Chen, J. G. *ChemSusChem* **2008**, *1*, 524.
(10) Skoplyak, O.; Barteau, M. A.; Chen, J. G. *J. Phys. Chem. B* **2006**, *110*, 1686.
(11) Medlin, J. W. *ACS Catal.* **2011**, *1*, 1284.
(12) Menning, C. A.; Chen, J. G. *J. Chem. Phys.* **2009**, *130*, 174709.
(13) Oyama, S. T. *The chemistry of transition metal carbides and nitrides*; Blackie Academic & Professional: Glasgow, 1996.
(14) Hwu, H. H.; Chen, J. G. *Chem. Rev.* **2005**, *105*, 185.
(15) Levy, R. B.; Boudart, M. *Science* **1973**, *181*, 547.
(16) Esposito, D. V.; Hunt, S. T.; Stottlemyer, A. L.; Dobson, K. D.; McCandless, B. E.; Birkmire, R. W.; Chen, J. G. *Angew. Chem., Int. Ed.* **2010**, *49*, 9859.
(17) Ren, H.; Hansgen, D. A.; Stottlemyer, A. L.; Kelly, T. G.; Chen, J. G. *ACS Catal.* **2011**, *1*, 390.
(18) Gouypailler, P.; Pauleau, Y. *J. Vac. Sci. Technol. A* **1993**, *11*, 96.
(19) Humbert, M. P.; Menning, C. A.; Chen, J. G. *J. Catal.* **2010**, *271*, 132.
(20) Kresse, G.; Furthmuller, J. *Phys. Rev. B* **1996**, *54*, 11169.
(21) Kresse, G.; Furthmuller, J. *Comput. Mater. Sci.* **1996**, *6*, 15.
(22) Kresse, G.; Hafner, J. *Phys. Rev. B* **1993**, *47*, 558.
(23) Perdew, J. P.; Chevary, J. A.; Vosko, S. H.; Jackson, K. A.; Pederson, M. R.; Singh, D. J.; Fiolhais, C. *Phys. Rev. B* **1992**, *46*, 6671.
(24) Teter, M. P.; Payne, M. C.; Allan, D. C. *Phys. Rev. B* **1989**, *40*, 12255.
(25) Hammer, B.; Norskov, J. K. *Adv. Catal.* **2000**, *45*, 71.

(26) Skoplyak, O.; Barteau, M. A.; Chen, J. G. *Catal. Today* **2009**, *147*, 150.
(27) Norton, P. R.; Davies, J. A.; Jackman, T. E. *Surf. Sci.* **1982**, *121*, 103.
(28) Ertl, G.; Neumann, M.; Streit, K. M. *Surf. Sci.* **1977**, *64*, 393.
(29) Jetzki, M.; Luckhaus, D.; Signorell, R. *Can. J. Chem.* **2004**, *82*, 915.
(30) Michelse., H; Klaboe, P. *J. Mol. Struct.* **1969**, *4*, 293.
(31) Salciccioli, M.; Yu, W.; Barteau, M. A.; Chen, J. G.; Vlachos, D. G. *J. Am. Chem. Soc.* **2011**, *133*, 7996.